CrossMark
click for updates

RSE-box:
An analysis and modelling package to study response times to multiple signals

Thomas U. Otto [a], ✉

[a]School of Psychology and Neuroscience, University of St. Andrews

Abstract ■ Responses to two redundant sensory signals are typically faster than responses to the individual component signals. This redundant signals effect (RSE) is extensively studied not only with an impressive variety of signals but also across different subject populations focusing on development, aging, and many clinical samples. Yet, a standardized methodology to analyse and interpret the RSE is not consistently employed. Moreover, an intriguing explanation of the effect, based on the so-called race model championed by Raab (1962), is typically not fully appreciated in its explanatory power. To facilitate RSE research, here, an analysis and modelling toolbox, called RSE-box, is introduced. It provides MATLAB functions that (1) perform basic analysis steps on response times (RTs), (2) investigate the RSE at the level of RT distributions, (3) fit the most recent race model by Otto and Mamassian (2012), and (4) simulate the RSE with synthetic data. The model functions are accompanied by parameter recovery simulations to test and validate the fitting procedures. An example of the simulation results is the demonstration that the analysis of group RT distributions can be biased. The RSE-box includes demonstration code and all functions are supported by help-documentation.

Keywords ■ multisensory processing, perceptual decision making, reaction time, model fitting and parameter recovery . **Tools** ■ MATLAB.

✉ to7@st-andrews.ac.uk

TUO: 0000-0002-8621-9462

Introduction

The combined use of different signals within and across sensory modalities is often beneficial. A classic example to study such benefits is the redundant signals paradigm (Kinchla, 1974; Miller, 1982; Todd, 1912). In two single signal conditions, participants are asked to respond on presentation of signal X and Y, respectively. In a third redundant signals condition, the two signals are presented together. The two signals are redundant in the sense that detection of either signal is sufficient for a correct response. A thorough analysis of the task demands shows that the paradigm combines two detection tasks, one for each signal, by a logical disjunction (Otto & Mamassian, 2017). The typical finding is that response times (RTs) to redundant signals XY are on average faster than RTs to the single signals, which is called the redundant signals effect (RSE; for a few recent examples, see Amsellem, Hochenberger, & Ohla, 2018; Crosse, Foxe, & Molholm, 2019; Fitousi & Algom, 2018; Freeman, Wood, & Bizley, 2018; Innes & Otto, 2019; Lunn, Sjoblom, Ward, Soto-Faraco, & Forster, 2019; Stefanou et al., 2019; Vrancken, Vermeulen, Germeys, & Verfaillie, 2019).

An intriguing explanation of the RSE is statistical facilitation (Raab, 1962). The basic idea is that signals X and Y are processed by two parallel decision units. On a given trial with redundant signals, a response can then be triggered by the unit that detects a signal first. If the distributions of detection times overlap, it is expected that responses to redundant signals are on average faster and less

variable compared to responses in the two single signal conditions. To implement statistical facilitation in a model, it is interesting to note that the coupling of the two parallel decision units is achieved by a logic OR gate, which implies that the model architecture perfectly matches the task demands of the redundant signals paradigm. Models incorporating this basic architecture are called race models. A powerful feature of Raab's (1962) proposal is that race models directly allow for predictions of the RT distribution with redundant signals, which can be computed based on the RT distributions in the two single signal conditions and probability summation. Miller (1982) used this feature to develop a test that checks if the RSE is in accordance with race model predictions. The test computes an upper bound under the assumption of a pure race process, meaning that the two parallel decision units do not interact (i.e., a unisensory decision process remains unchanged whether or not a second signal is present). In a more technical language, the test assumes context invariance (e.g., Ashby & Townsend, 1986; Colonius, 1990; Luce, 1986; Townsend & Wenger, 2004). Interestingly, this so-called Miller's bound is often found to be violated, which has led to a widespread rejection of race models as an explanation of the RSE.

The rejection of race models is however not always watertight. For example, Gondan and Minakata (2016) reviewed 83 studies between 2011 and 2014 that used Miller's test. Of these, 77 studies (93%) claimed violations of Miller's bound, which seems to suggest that race models can safely be rejected. However, 24 studies (29%) have actually not used the upper bound as developed by Miller (1982) but what is called the independent race model prediction (for more details, compare Equations 6 and 7 below). The consequence of this methodological inconsistency is that this subset of studies in fact lacks the critical test, which would be needed to support Miller's (1982) conclusion. Even more problematic, only 9 studies (11%) presented an alternative model to describe and predict their data. Hence, the majority of studies rejects race models as an explanation of the RSE but does not provide an alternative account that allows for testable predictions.

A further key issue is that the context invariance assumption is made when Miller's bound is computed. As context invariance is not necessarily true (Luce, 1986), it is well possible that violations of Miller's bound occur because the context invariance assumption is wrong. It follows that the test using Miller's bound is limited to pure race models without any interaction between the parallel decision units. In contrast, the test is mute about race models that allow for interactions. Given that the context invariance assumption is frequently not even mentioned when testing the RSE with Miller's bound, it seems that the explanatory power of race models is largely underestimated in RSE research.

This gap was explored by Otto and Mamassian (2012), who returned to the race model architecture championed by Raab (1962). Firstly, the authors showed that models of the RSE should consider the sequential dependency of RTs in the redundant signals paradigm. Such history effects were already reported by Miller (1982) but are often not investigated in RSE studies. Secondly, to account for violations of Miller's bound, Otto and Mamassian (2012) proposed an unspecific noise interaction to model a potential violation of the context invariance assumption. Specifically, models of perceptual decision making assume that sensory evidence is accumulated over time until a response criterion is reached, a process that is corrupted by noise (e.g., Bogacz, 2007; Forstmann, Ratcliff, & Wagenmakers, 2016; Gold & Shadlen, 2007). The proposed idea is that the noise level may not be constant but increasing when the context is changed from single to redundant stimulation. Strikingly, adding noise as an interaction parameter made this race model one of the very few to account for the RSE including violations of Miller's bound at the level of RT distributions. This work demonstrates that the basic race model architecture shows in fact strong explanatory power.

To facilitate investigation of the RSE and involved processing interactions, here, an analysis and modelling toolbox, named RSE-box, is introduced. The material is organised in two main sections. To cover key steps when approaching the RSE, a first section discusses RSE-box functions that (1) perform basic analysis steps on RTs, (2) investigate the RSE at the level of RT distributions, (3) fit the most recent race model by Otto and Mamassian (2012), and (4) simulate the RSE with synthetic data. To validate the implemented model fitting procedures, a second section presents model simulations to check parameter recovery performance. These simulations also test methods that are frequently used for the removal of RT outliers and the extraction of group RT distributions.

RSE-box functions

The RSE-box is implemented in MATLAB (MathWorks, Inc.) and is available as Supplementary Material attached to this article. With additional functions and updates, it is also available for download at: https://github.com/tomotto/RSE-box/. For installation, please copy the toolbox to your computer and add the folder containing the RSE-box (including subfolders) to the MATLAB path. As a prerequisite, some toolbox functions require MATLAB's Statistics and Machine Learning Toolbox. Table 1 provides an overview of RSE-box functions, which are discussed in detail in the following. All toolbox functions are accompanied by help

Table 1 ∎ Overview of discussed RSE-box functions

Section	Function name	Description
Defining RT distributions	getCP	Computation of cumulative probabilities
	interpCDF	Linear interpolation of an empirical CDF
	outCorrect	Outlier correction
	sampleDown	Down-sampling of an empirical CDF
Quantifying the RSE	getGain	Computation of redundancy gain (the RSE)
	getViolation	Computation of Miller's bound violation
	getRaab	Computation of Raab's independent race model
	getGrice	Computation of Grice's bound (max. positive correlation)
	getMiller	Computation of Miller's bound (max. negative correlation)
	fillArea	Fill the area between two CDFs (plotting tool)
Modelling RTs to single signals	fitLater	Fitting of the LATER model (2 parameters)
	bootLater	Bootstrapping 95% confidence intervals for LATER model fits
	laterCDF	LATER model, reci-normal CDF (plotting tool)
Modelling RTs to redundant signals	fitRace	Maximum likelihood estimation (MLE) of a race model
	bootRace	Bootstrapping 95% confidence intervals for race model fits
	raceCDF	Race model CDF (plotting tool)
Modelling RTs in all RSE conditions	fitRse	Fitting of all 3 RSE conditions (6 parameters)
	bootRse	Bootstrapping 95% confidence intervals for model fits
	fitRseRaab	MLE of the independent race model (4 parameters)
	fitRseEta	MLE of the race model (5 parameters)
	fitRseRho	MLE of the race model (5 parameters)
Simulating the RSE	simLater	Simulation of RTs using the LATER model
	simRace	Simulation of RSE data with a race model
Demonstration code	demo01_quantiles	Demonstration of analysis steps as shown in Figures 2 and 3
	demo02_later	Demonstration of analysis steps as shown in Figure 4
	demo03_race	Demonstration of analysis steps as shown in Figure 5

Note. The RSE-box function documentation provides more detailed descriptions, which can be accessed by typing for example `help getRaab` in MATLAB's command window (Figure 1). Note that some functions require MATLAB's Statistics and Machine Learning Toolbox.

documentation, which can be accessed by typing `help functionName` in MATLAB's command window (Figure 1). The functionality of the RSE-box is guided by demonstration code (see Appendix for an example), which illustrates the analysis steps shown in Figures 2-5.

Defining RT distributions

An analysis of RTs may just focus on measures of central tendency. For example, the RSE can be described as the decrease of mean RT in redundant compared to single signal conditions. However, it is well established that underlying cognitive processes can be studied in more detail by considering RT distributions (Luce, 1986). Additional RT characteristics include for example the large spread and the positive skew of the distributions. Initiated by Miller (1982), research on the RSE has a longstanding tradition to consider RT distributions. The description of the RSE-box consequently starts with procedures to visualize the RSE at the level of RT distributions.

The RSE is typically tested with highly salient signals, which means that detection performance is expected to be at ceiling (hardly any signal should be missed, the false alarm rate should be low). It is important to note that the analysis and modelling procedures described here assume ceiling performance. As a first analysis step, it is therefore recommended to check actual performance levels in terms of miss and false alarm rates. It may be appropriate to exclude participants with high error rates. If the assumption of ceiling performance is generally violated, the analysis and modelling procedures, as presented here, need to be adapted to account for error rates (see also Gondan & Minakata, 2016).

RSE experiments are typically performed in long-lasting sessions to collect large numbers of trials, which is required for an analysis of RT distributions. As behavioural performance is susceptible to attentional lapses,
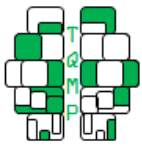
The Quantitative Methods for Psychology

Figure 1 ■ RSE-box function documentation. All RSE-box functions are accompanied by help documentation, which can be accessed by typing help functionName in MATLAB's command window. The documentation provides a description of the computation performed by the function including in- and output variables, references when appropriate, and links to the documentation of related functions. The example shows the documentation of the function `getRaab` that computes Raab's (1962) independent race model predication (for an overview of discussed RSE-box functions, see Table 1).

```
>> help getRaab
getRaab   Computation of Raab's independent race model.
 [RAAB, P] = getRaab(DATA) returns Raab's independent race
 model prediction to analyse a redundant signals experiment
 (Raab, 1962). Input argument DATA is an N-by-2 matrix that
 contains reaction times in the two single signal conditions
 (if DATA has more than two columns, columns 1 and 2 are
 used). The output argument RAAB is a time vector that
 defines the model prediction. The output argument P provides
 corresponding cumulative probabilities.

 Reference:
 Raab (1962). Statistical Facilitation of Simple Reaction
 Times. Transactions of the New York Academy of Sciences,
 24(5), 574-590.

 See also demo01_quantiles, getCP, getGain, sampleDown
```

an outlier correction can be used to remove extreme values from the data. While in some contexts an outlier correction is not advocated (c.f., Luce, 1986), it is here recommended to perform a cleaning separately for each condition and participant (see 'Error contamination and outlier correction' below). The RSE-box includes the function `outCorrect` that uses the absolute deviation around the median as criterion (Leys, Ley, Klein, Bernard, & Licata, 2013). To account for the skewed nature of RTs, the function first transforms RTs into rates (1/RT). It then excludes data points that deviate by more than 1.4826 * 3 median absolute deviations (MADs) from the median rate. This criterion corresponds to 3 standard deviations (SDs) if rates are

normally distributed. Consequently, the criterion is conservative in the sense that it is expected to exclude only about 0.27% of the data points. Actual exclusion numbers can be higher, for example, if performance is contaminated by frequent false alarms.

To visualize RT distributions, it is standard in RSE research to inspect cumulative distribution functions (CDFs). For this, the proportions of observed response need to be translated into probabilities, which can be obtained in a two-step procedure. First, valid RTs collected from one participant in a given condition are stored as a vector, which is sorted from the fastest to the slowest (e.g., using MATLAB's sort command; Figure 2a). For example, if N valid

Table 2 ■ RSE simulation and parameter recovery

Signal condition	Model	Parameter	Unit	Simulation, true value*	Recovery, best-fit**	Joint recovery, best-fit
Single X	LATER model	μ_x	s^{-1}	2.5	2.48	2.49
		σ_x	s^{-1}	0.4	0.367	0.365
Single Y	LATER model	μ_y	s^{-1}	2.5	2.46	2.47
		σ_y	s^{-1}	0.4	0.419	0.414
Redundant XY	Race model	ρ		-0.5	-0.458	-0.431
		η	s^{-1}	0.1	0.137	0.134

Note. * The parameter values were used to generate the data shown in Figure 2c. ** Fitting is performed in two steps. Corresponding distributions are shown in Figure 4 and Figure 5.

Figure 2 ■ Plotting RT data as cumulative distribution functions (CDFs). a) A vector of response times (RTs) is sorted from the fastest to the slowest. b) Cumulative probabilities are assigned based on ranks using Equation 1. c) CDFs for the three RSE conditions are obtained by plotting the sorted RTs against the assigned cumulative probabilities. Continuous distributions are obtained by linear interpolation. Synthetic data, see section 'Simulating the RSE'.
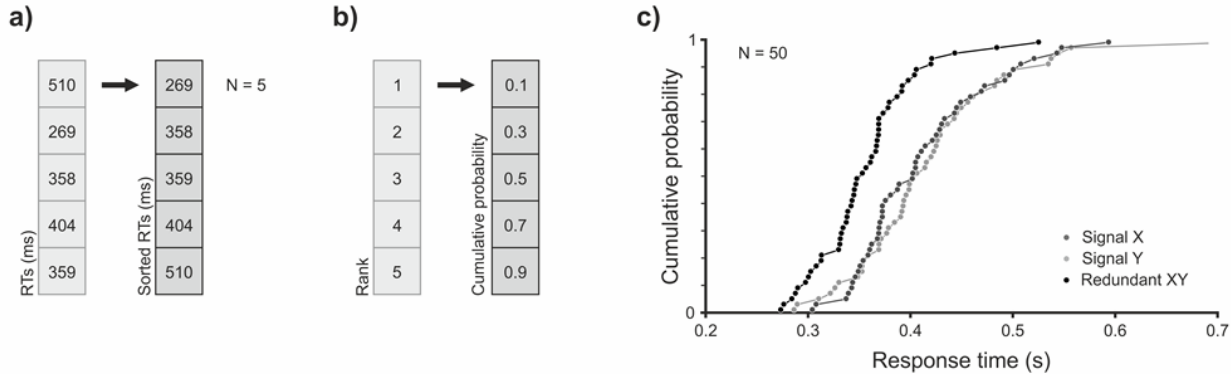
RTs to signal X are collected, this yields a vector X_i, where i indicates the rank ranging from 1 to N. Then, a vector of corresponding cumulative probabilities P_i can be computed by

$$P_i = \frac{i - 0.5}{N} \qquad (1)$$

based on the ranks i (Figure 2b). Note that Equation 1 assigns a cumulative probability of 0.5 to the median in agreement with its definition. The RSE-box includes the function `getCP` that computes cumulative probabilities using Equation 1. To visualize the RSE, the sorted RTs in each condition are plotted against the corresponding cumulative probabilities (Figure 2c). When inspecting CDFs, the RSE is eminent in that the RT distribution with redundant signals is shifted to the left (towards faster RTs) and is faster rising (with smaller variance) compared to the single signal conditions.

To make predictions of the RSE using race models, as we will see below, it is a key step to obtain continuous distribution functions from the discrete RT samples. One straightforward solution is linear interpolation, which does not require distributional assumptions. Such assumptions are made when for example the LATER model (Linear Approach to Threshold with Ergodic Rate model; Carpenter & Williams, 1995; Noorani & Carpenter, 2016); or an ex-Gaussian distribution (Heathcote, Popiel, & Mewhort, 1991; Luce, 1986) is used to fit RTs in the single signal conditions. The RSE-box includes the function `interpCDF` that performs linear interpolation (see connecting lines in Figure 2c). Furthermore, to measure the size of the RSE and to quantify race model predictions, some computations can

be simplified if the number of data points is the same in the three RSE conditions. However, depending on performance and procedures (including for example an outlier correction), the number of valid RTs typically differs across conditions and participants. To extract equal numbers of quantile RTs, the RSE-box includes the function `sampleDown`, which performs a down-sampling of empirical CDFs using linear interpolation. For example, Innes and Otto (2019) collected 100 trials per participant and condition, which yielded variable numbers of valid RTs after data cleaning. The authors then down-sampled each distribution to 50 quantile RTs to quantify the RSE as described next.

Quantifying the RSE

Obviously, a first step of the RSE analysis is to measure the size of the effect. At the level of RT distributions, the RSE corresponds to the area enclosed by the CDF of the redundant signals conditions and the faster CDF of the two single signal conditions (Figure 3a; Otto, Dassy, & Mamassian, 2013; for related geometric measures, see Colonius & Diederich, 2006; Miller, 1986). The latter corresponds to the so-called Grice's bound, which is the lower bound for race models that assume context invariance (Grice, Canham, & Gwynne, 1984; Townsend & Wenger, 2004). Grice's bound corresponds to the race model prediction assuming a maximal positive correlation between processing times for signals X and Y (Colonius, 1990). It can be computed by

$$P_{\text{Grice}}(t) = \max\left(P_X(t),\ P_Y(t)\right), \qquad (2)$$

Figure 3 ■ Quantifying the RSE. Both panels show the same synthetic data as Figure 2c. a) To measure the RSE at the level of RT distributions, Grice's bound is taken as reference, which is given by the faster of the CDFs in the single signal conditions (Equation 3). The RSE is then given by the area enclosed by the CDF with redundant signals and Grice's bound (Equation 5). b) To compute Miller's bound, the CDFs in the two single signal conditions are summed (Equation 7). Violations of Miller's bound occur when the CDF with redundant signals is above Miller's bound. Violations can be quantified by the area enclosed by the two curves (Equation 11).
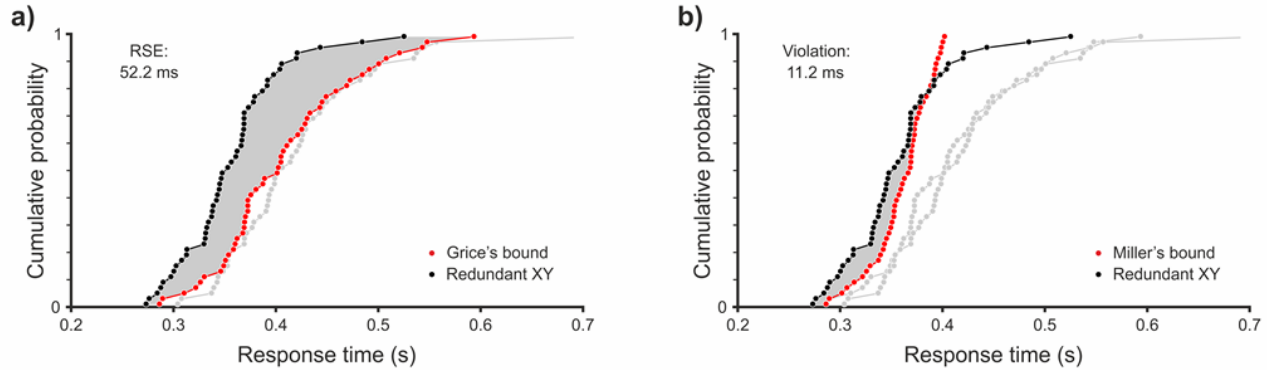
where $P_X(t)$ and $P_Y(t)$ describe the CDFs in the single signal conditions with signals X and Y, respectively. With empirical distributions, each CDF is given by a sorted vector of RTs (Figure 2a). If the vectors X_i and Y_i have the same length N, the computation of Grice's bound can be simplified by selecting the faster of the two RTs at each rank i (ranging from 1 to N)

$$\text{Grice}_i = \min\left(X_i, \ Y_i\right). \tag{3}$$

The RSE-box function `getGrice` computes Grice's bound using Equation 3 (the function `sampleDown` can be used to obtain the same number of RT quantiles in the two single signal conditions, see above). Grice's bound can be visualized by plotting the RT quantiles given by the vector Grice$_i$ against corresponding cumulative probabilities (Figure 3a).

With Grice's bound as reference, the size of the RSE can be measured by the size of the area enclosed by the CDF in the redundant signal condition $P_{XY}(t)$ and Grice's bound $P_{\text{Grice}}(t)$ as defined in Equation 2 (Otto et al., 2013). Thus, the size of the RSE can be computed by

$$RSE = \int_T \left(P_{XY}\left(t\right) - P_{Grice}\left(t\right)\right) \mathrm{d}t, \tag{4}$$

where the integral is the definite integral taken for response time t ranging over the set of possible response times T. If empirical CDFs are based on the same number of RTs in each condition (see above), the measurement

of the RSE can be approximated by averaging the differences between the RTs in the redundant signal condition and Grice's bound at each rank i (ranging from 1 to N)

$$RSE = \frac{\sum Grice_i - XY_i}{N}, \tag{5}$$

where XY_i is the sorted vector of RTs in the redundant signals condition and Grice$_i$ the bound as computed in Equation 3. It should be noted that the size of the RSE as computed in Equation 5 is the same as the difference in mean RTs between the redundant and the faster of the two single signal conditions if the CDF in one single signal condition is stochastically dominant (i.e., one CDF is always above the other; Heathcote, Brown, Wagenmakers, & Eidels, 2010). However, empirical CDFs are frequently crossing, which is considered in Equation 5 to measure the RSE at the level of RT distributions. The RSE-box function `getGain` computes the size of the RSE following Equations 3 and 5 taking only the empirical RT data as input. The RSE-box function `fillArea` can be used to highlight the area corresponding to the RSE (as shown in Figure 3a).

In many experiments, the RSE is tested with different signal types and intensities as well as different subject populations including many clinical samples (for a methods review covering 181 related papers, see Gondan & Minakata, 2016). From the analysis of race models, it is expected that the size of the RSE depends on behavioural performance in the single signal conditions (Otto et al., 2013). Firstly, the RSE is expected to be larger when behavioural perfor-

mance in the two single signal conditions is similar (principle of equal effectiveness). Secondly, the RSE is expected to scale with the spread of RTs in the single signal conditions (variability rule). To understand any difference in the size of the RSE that is expected from differences in unisensory performance levels, a first step is to look at the predictions made by Raab's (1962) race model, which is the most basic race model to account for the RSE. It simply assumes that a response in redundant conditions is triggered by the faster of two parallel decision processes (one for each signal). The model allows for direct predictions of RT distributions with redundant signals using probability summation

$$P_{\text{Raab}}(t) = P_X(t) + P_Y(t) - P_X(t) * P_Y(t), \quad (6)$$

where $P_X(t)$ and $P_Y(t)$ describe the CDFs in single signal conditions with signals X and Y, respectively. It is important to note that the model assumes statistical independence between processing times of the two signals, for what reason it is also called the independent race model. It also assumes context invariance (Ashby & Townsend, 1986; Colonius, 1990; Luce, 1986; Townsend & Wenger, 2004), which is a hidden assumption that must be considered if inferences are made based on race model predictions (a detailed analysis of this critical issue is provided by Otto & Mamassian, 2017). The RSE-box contains the function getRaab that computes the independent race model prediction in accordance with Equation 6. Analogously to the function getGrice (see above), it requires the same number N of RTs in both single signal conditions as input. It returns a vector of RT quantiles, here called Raab$_i$, which describes the independent race model prediction with N quantiles. The prediction can be visualized by plotting the vector Raab$_i$ against the corresponding cumulative probabilities. To quantify the size of the RSE as predicted by Raab's (1962) independent race model, the same approach as in the measurement of the empirical RSE can be applied (Equation 5; instead of the empirical RTs in the redundant conditions XY_i, the prediction Raab$_i$ is substituted; see also RSE-box function getGain). These computations provide simple, parameter-free predictions of the expected RSE.

The independent race model predictions are highly useful to access if a difference in RSE may be expected due to changes in unisensory performance levels. For example, consider an imagined clinical study that compares the RSE across two groups. The clinical group may show overall slower and more variable RTs than the control group, which may point to some deficit associated with the clinical condition. The RSE however may be larger in the clinical group, which consequently may point to a paradoxical benefit. Critically, checking the race model predictions would solve the paradox. In the example here, a larger

RSE is simply expected because of the increased variability of unisensory RTs in the clinical group (see variability rule, Otto et al., 2013). When testing the RSE across different subject populations or signal types and intensities, it is here recommended to check if the independent race model would predict differences in RSE.

Historically, research on the RSE has very much focused on the upper limit of the RSE that is still in agreement with the parallel processing architecture as assumed by race models. In a milestone contribution, Miller (1982) pointed out that race model predictions can exceed Raab's (1962) model if the assumption of statistical independence is dropped. In fact, an upper bound can be computed by

$$P_{\text{Miller}}(t) = P_X(t) + P_Y(t), \quad (7)$$

where $P_X(t)$ and $P_Y(t)$ describe the CDFs in single signal conditions with signals X and Y, respectively. This so-called Miller's bound still assumes context invariance. It corresponds to the race model prediction assuming a maximal negative correlation between processing times for signals X and Y (Colonius, 1990). The RSE-box function getMiller computes Miller's bound in accordance with Equation 7. The computation basically follows the algorithm by Ulrich, Miller, and Schröter (2007), but is implemented differently. Analogously to the functions getGrice and getRaab (see above), it requires the same number N of RTs in both single signal conditions as input. It returns a vector of RT quantiles, called Miller$_i$, which describes Miller's bound with N quantiles. The bound can be visualized by plotting the vector Miller$_i$ against the corresponding cumulative probabilities (Figure 3b).

Inspection of Miller's bound is interesting as it allows for inferences about the processing of sensory signals when tested in the redundant signals paradigm. Miller (1982) argued that the RT distribution with redundant signals cannot surpass Miller's bound if a race model underlies the RSE. This implication can be expressed as an inequality

$$P_{XY}(t) \leq P_{\text{Miller}}(t), \quad (8)$$

where $P_{XY}(t)$ describes the CDF in the redundant signals condition and $P_{\text{Miller}}(t)$ is Miller's bound as computed by Equation 7. To reject race models as an explanation of the RSE, following the modus tollens, it needs to be shown that Inequality 8 is violated. There are several ways to test for such violations. A frequently used approach is to check if RTs in the redundant signals condition, given by the vector XY_i, violate Miller's bound at any rank i (ranging from 1 to N). For this purpose, Inequality 8 can be re-written as

$$XY_i \geq \text{Miller}_i, \quad (9)$$

where Miller$_i$ is the vector of RT quantiles defining Miller's bound (which can be obtained from the RSE-box function

getMiller, see above). An issue to consider with this approach is that statistical tests are computed at several ranks and that multiple testing inflates Type I error rates (Gondan, 2010; Kiesel, Miller, & Ulrich, 2007).

An alternative approach proposed by Colonius and Diederich (2006) measures the size of the area between Miller's bound and the RT distribution with redundant signals when Inequality 8 is violated. This violation area can be computed by

$$Violation = \int_T \max\left(P_{XY}\left(t\right) - P_{\text{miller}}\left(t\right), 0\right) dt, \quad (10)$$

where the integral is the definite integral taken for response time t ranging over the set of possible response times T. Note that this approach is similar to the computation of the size of the RSE (see Equation 4). Consequently, as with the measurement of the RSE, the computation of the violation area can be simplified if distributions are based on the same number N of RTs in each condition

$$Violation = \frac{\sum max\left(\text{Miller}_i - XY_i, 0\right)}{N}. \quad (11)$$

The RSE-box function getViolation quantifies the size of the violation area using Equation 11. The RSE-box function fillArea can be used to highlight the violation area (as shown in Figure 3b). Interestingly, violations of Miller's inequality are frequently found in RSE experiments, which implies that some sort of interaction has occurred in the simultaneous processing of the tested signals.

At this point it is important to remind a critical issue when interpreting the test. Like Raab's (1962) independent model, Miller's (1982) bound assumes context invariance, which is however not necessarily true (Luce, 1986). Consequently, it is a fallacy to deduce from violations of Miller's bound that all race models can be rejected. A valid alternative is that the basic architecture of race models is correct, but that the context invariance assumption is wrong (for a careful deconstruction of the argument, see Otto & Massian, 2017; see also Yang, Altieri, & Little, 2018). In an evaluation of the RSE using Miller's test, it is therefore vital to check if the context invariance assumption is properly considered. If the possibility of context variant race models is not taken into account, conclusions must be viewed with reservation.

To summarize the material so far, RSE research has a longstanding tradition to work with RT distributions. The standard approach is easy to perform at the level of empirical RTs, and the RSE-box provides functions for the analysis steps that are required, for example, to quantify the RSE or to measure violations of Miller's bound (Figure 3). When testing across different signal types or intensities

as well as across different subject populations, a recommended new analysis is to check if Raab's (1962) independent race model would predict differences in RSE, which is a vital assessment before interpreting any difference in RSE. A convenient feature of the standard approach is that it requires no distributional assumptions and that all computations are directly based on the empirical RTs. As one of the shortcomings, the approach does only allow to conclude that some sort of interaction has occurred in the simultaneous processing of the tested signals. To investigate and understand these interactions in more detail, a model-based approach is needed that analyses and explains the entire distribution of RTs to redundant signals (Otto & Massian, 2017). Such a modelling approach typically requires distributional assumptions to describe RTs in the single signal conditions. To introduce corresponding fitting procedures, the next section first presents the RSE-box functions that describe unisensory RT distributions using the LATER model (Carpenter & Williams, 1995; Noorani & Carpenter, 2016), which is a prerequisite to then model RT distributions with redundant signals.

Modelling RTs to single signals

With unisensory signals, models of perceptual decision making assume that noisy evidence for a sensory signal is accumulated over time until a threshold is reached, in which case a categorical decision is made and a corresponding motor response is triggered (e.g., Bogacz, 2007; Forstmann et al., 2016; Gold & Shadlen, 2007). These features are covered by the LATER model (Carpenter & Williams, 1995; Noorani & Carpenter, 2016), which approximates the noisy evidence accumulation by sampling a drift rate from a normal distribution (Figure 4a). A response is triggered when the accumulated evidence reaches a threshold (which can be arbitrarily set to 1). On presentation of signal X, the model consequently assumes that an RT distribution is given by the reciprocal of a normally distributed drift rate distribution ($1/D_X$, where D_X follows a normal distribution with mean μ_X and standard deviation σ_X). The resulting reci-normal distribution is skewed to the right similar to empirical RT distributions (the term "reci-normal" comes from the contraction of "reciprocal" and "normal").

The LATER model can be used to obtain continuous distribution functions in the single signal conditions. For this, RTs are transformed into rates (1/RT), which can then be described by fitting a normal distribution. The RSE-box function fitLater performs these two steps and returns the minimum variance unbiased estimators (MVUEs) of the two parameters μ and σ of the rate distribution. With the best-fitting parameter estimates, the function laterCDF can be used to plot the corresponding RT distribution (Fig-

Figure 4 ∎ Modelling RTs to single signals. a) LATER model. On presentation of signal X, evidence for the signal is accumulated starting at level L_0. A response is triggered when the threshold L_T is reached. The drift rate D_X is subject to noise, which is modelled by a normal distribution (an exemplary trial is indicated by the line ending in a dot). The resulting RT distribution follows the reciprocal of D_X, which is a reci-normal distribution (here shown as PDF). b) RTs to single signal X (identical data as shown in Figure 2c). The solid green line is the CDF of the best fitting LATER model with free parameters μ_X and σ_X (see Table 2 for best-fitting estimates). The shaded area indicates 95% confidence intervals as calculated by 1,000 repetitions of a bootstrap procedure.
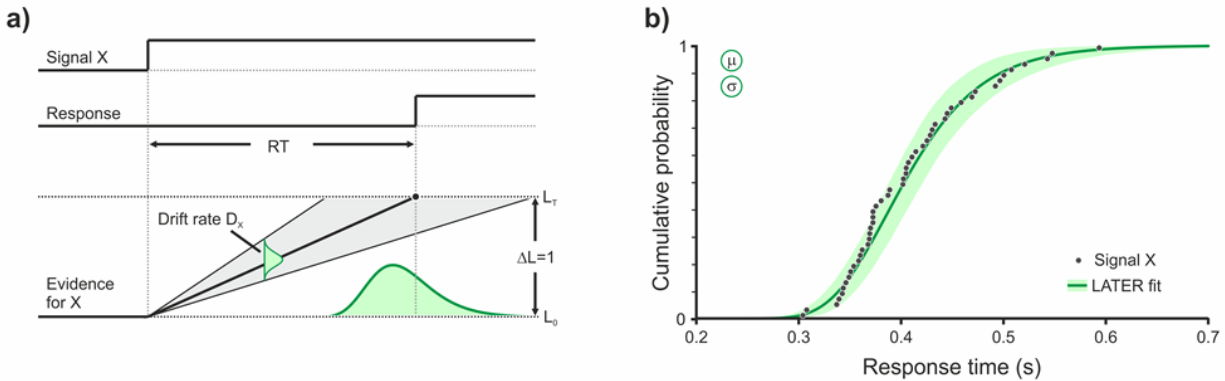
ure 4b). Finally, using bootstrapping (Efron & Tibshirani, 1994), the function `bootLater` computes 95% confidence intervals for the best-fitting parameter estimates as well as for the resulting CDF. The latter can be plotted using the function `fillArea` (Figure 4b). As we will see next, using the LATER model to describe RTs in the single signal conditions is a convenient choice to model the RSE within the race model framework.

Modelling RTs to redundant signals

Race models assume that a response to redundant signals is triggered by the faster of two parallel decision processes (one for each component signal). As shown by Raab (1962), this basic architecture readily predicts a speed-up of responses to redundant signals due to statistical facilitation. To implement a race model, Otto and Mamassian (2012) used a logic OR gate to map the two LATER units to a single motor output (Figure 5a). When assuming context invariance, the two LATER units are fully constrained by the RTs in the single signal conditions. With this basic architecture, a response to redundant signals is triggered by the faster of two LATER units, which is set by the unit with the larger drift rate on a given trial. Conveniently, the exact distribution of the maximum of two normally distributed random numbers is known (Nadarajah & Kotz, 2008), which allows direct computation of race model predictions at the level of RT distributions.

As pointed out by (Miller, 1982), RTs as measured in single signal conditions cannot be assumed to be statistically independent. For example, one issue is that the three conditions of the redundant signals paradigm are typically randomly interleaved in experiments. Crucially, RTs in single signal conditions show sequential dependency, with faster responses following modality repetitions compared to modality switches (e.g., Gondan, Lange, Rösler, & Röder, 2004; Miller, 1982, 1986; Otto & Mamassian, 2012). At least for this reason, it is important to consider potential correlations when computing race model predictions. Following the classic approach, predictions were computed assuming statistical independence (Raab's independent race model, Equation 6) or assuming extreme correlations of -1 and 1 (Miller's and Grice's bounds, Equations 7 and 2). In contrast, the maximum distribution of two normally distributed random numbers can be computed for any correlation ρ (Nadarajah & Kotz, 2008). Thus, a convenient advantage of the new approach is that it allows for predictions at the level of RT distributions for any correlation ρ (for an illustration of the effect of ρ on predictions, see Otto & Mamassian, 2012, their Fig. S2a).

Another issue is that RTs to redundant signals frequently violate Miller's bound (as illustrated in Figure 3b). As discussed above, such findings imply that some sort of interaction must occur in the processing of redundant signals (either the parallel architecture of race models or the context invariance assumption is wrong). Otto and Mamassian (2012) included a violation of the context invari-

Figure 5 ■ Modelling RTs to redundant signals. a) Basic race model architecture. On presentation of redundant signals XY, evidence for both signals is accumulated in parallel (here by two LATER units; see also Figure 4). A response is triggered when the first unit detects a signal, which is modelled by an OR gate. b) RTs to redundant signals XY (identical data as shown in Figure 2c). The solid red line is the CDF of the best fitting race model as proposed by Otto and Mamassian (2012) with free parameters ρ and η (see Table 2 for best-fitting estimates). The model is constrained by the LATER units as fitted in the two single signal conditions (dotted lines). The shaded area indicates 95% confidence intervals as calculated by 1,000 repetitions of a bootstrap procedure.
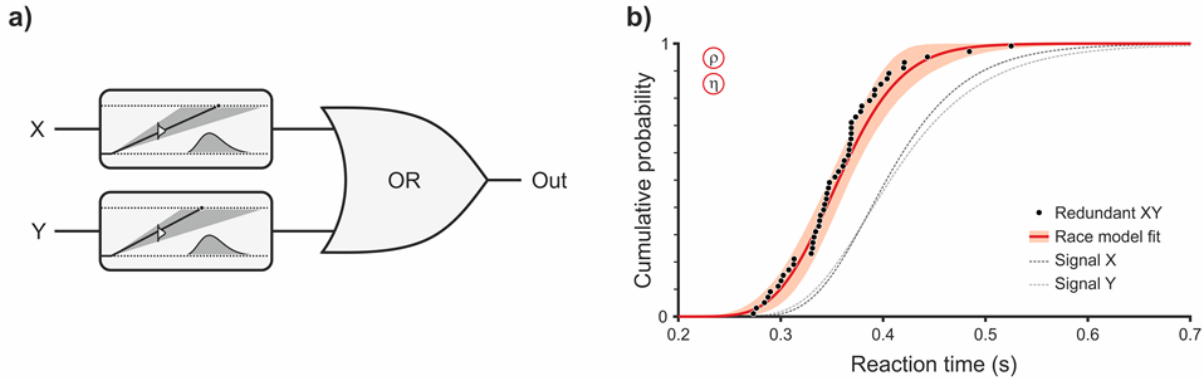
ance assumption in their model by allowing for an unspecific noise interaction during parallel evidence accumulation. The violation is implemented in the redundant signals condition by adding the noise η to the LATER model parameters σ_X and σ_Y as estimated in the two single signal conditions (for an illustration of the effect of η on predictions, see Otto & Mamassian, 2012, their Fig. S2b). An interesting outcome of additional noise is a speed-up of RTs at the fast tail of the distribution (leading to violations of Miller's bound), which comes however at the cost of a slow-down of RTs at the slow tail. Critically, any such effect is missed by the classic approach focusing on Miller's test, which is mute about the slow tail.

The context variant race model proposed by Otto and Mamassian (2012) can be used to fit RT distributions with redundant signals. The model is constrained by the two LATER units as fitted in the single signal conditions. Using maximum likelihood estimation (MLE; for a tutorial, see Myung, 2003), the RSE-box function `fitRace` computes best-fitting estimates of the two free model parameters ρ and η. With the best-fitting parameter estimates, the function `raceCDF` can be used to plot the corresponding RT distribution with redundant signals (Figure 5b). Finally, using bootstrapping (Efron & Tibshirani, 1994), the function `bootRace` computes 95% confidence intervals for the best-fitting parameter estimates as well as for the resulting race model CDF. As with the LATER model, the latter can be plotted using the function `fillArea` (Figure 5b).

Modelling RTs in all RSE conditions

The modelling approach has so far followed the two-step approach that historically developed from Miller's (1982) race model test. The first step obtains continuous distribution functions to describe the single signal conditions. Then, the second step uses these functions to obtain race model predictions for the redundant signals condition. An issue with this approach is that race model predictions inherit any sampling error from the first step. Moreover, any systematic mis-fit of the unisensory models automatically propagates to the race model predictions. Such issues should be considered when evaluating the model fit in the redundant signal conditions (e.g., when comparing the fit with alternative models).

To build an overall model that eases model comparison, the two-step approach can be reduced to a single modelling step that simultaneously fits all three conditions of the redundant signals paradigm. The RSE-box includes the function `fitRse`, which simultaneously fits the race model and the two LATER units to all data by maximizing the likelihood across conditions (Table 2, joint recovery). Using the best-fitting estimates of the six free parameters (μ_X, σ_X, μ_Y, σ_Y, ρ, and η), the functions `laterCDF` and `raceCDF` can be used to plot the corresponding three CDFs as demonstrated in Figure 4b and Figure 5b, respectively. The function `fitRse` also returns the maximized likelihood, which can be used to compare the race model

as implemented here with alternative models of the RSE, using for example the Akaike Information Criterion (AIC; Akaike, 1973) or the Bayesian Information Criterion (BIC, Schwarz, 1978; ; for tutorials on model selection, see Hélie, 2006; Pitt & Myung, 2002). The RSE-box includes also the additional functions `fitRseRho`, `fitRseEta`, and `fitRseRaab`, which are nested models with a reduced parameter space (assuming η, ρ, or both to be 0). Finally, as with the model functions above, the function `bootRse` computes 95% confidence intervals for the best-fitting parameter estimates as well as for the model CDFs.

Simulating the RSE

The RSE-box contains not only analysis and modelling functions but also functions to simulate the RSE. First, the function `simLater` simulates RTs in the single signal conditions by randomly sampling from a LATER model. Second, the function `simRace` simulates all three conditions of the redundant signals paradigm using the race model as proposed by Otto and Mamassian (2012). In fact, the data set to illustrate the toolbox functions (see Figure 2c) was generated using this function with the parameters as specified in Table 2. As the data were generated by a race model, the simulation effectively demonstrates that violations of Miller's bound do not allow rejecting all race models as an explanation of the RSE. Such synthetic data can be very useful to scrutinize analysis and modelling procedures as exemplified in the next section.

Simulation studies

Parameter recovery

It is good practice to test model fitting procedures by parameter recovery simulations (for an introduction, see Heathcote, Brown, & Wagenmakers, 2015). The basic idea is to first generate random data samples from a model. The synthetic data is then analysed in the same way as real data by fitting the model back to the data samples. The key difference to real data is that the true parameter values of the model that generated the synthetic data are known. This way, parameter recovery simulations can reveal potential systematic deviations from true values (biases) and provide a measure of the uncertainty associated with the recovered estimates (reliability). To validate the procedures, the aim is of course that the true parameter values are recovered unbiased.

To put the fitting procedures of the RSE-box to test, the parameter recovery simulation here tested 250 versions of the model as introduced by Otto and Mamassian (2012) (Figure 6a). To generate different model parameterizations, the values of the six parameters (μ_X, μ_Y, σ_X, σ_Y, ρ, and η) were randomly sampled from uniform distribu-

tions. The LATER model parameters μ_X and μ_Y were randomly selected with values between 2.0 and 2.5 s^{-1}. Consequently, expected median RTs in the single signal conditions varied between 0.4 and 0.5 s. More critically, due to the independent parameterization of the two LATER units, the difference in median RTs in the single signal conditions could vary between 0 and 0.1 s. The LATER model parameters σ_X and σ_Y were randomly sampled between 0.4 and 0.6 s^{-1}. Consequently, the MAD of RTs could vary roughly between 0.04 to 0.1 s in the single signal conditions . The race model parameter ρ varied between 1 and -1. With the former value, no RSE is expected (see Grice's bound, Equation 2). With the latter value, the maximal possible RSE under the assumption of context invariance is expected (see Miller's bound, Equation 7). Finally, the race model parameter η varied between 0 and 0.2 s−1. Consequently, the model versions could yield either no violation of Miller's bound (context invariance holds) or violations of up to 0.024 s, which is more than typically reported in empirical RSE studies (for comparison, Figure 3b shows a violation of 0.011 s). With the overall parameterization, the simulated RSE could range between about 0 and 0.1 s, which covers most empirical RSE studies (for comparison, Figure 3a shows an RSE of 0.052 s). Each model version was then used to simulate an RSE experiment 2,000 times (Figure 6a). For each simulation, 100 RTs for each of the three conditions were randomly sampled using the RSE-box function `simRace`. The synthetic data samples were then analysed using the function `fitRse` to obtain best fitting estimates of the six model parameters using MLE.

Visual inspection of the recovery performance reveals that the fitting procedure provides fairly unbiased parameter estimates throughout the wide range of tested values (Figure 6b-e). Recovery of the LATER model parameter μ is unbiased (Figure 6b). There is some variance in the reliability of the parameter estimates as indicated by the spiky shape of the area depicting the interquartile range (IQR). This variance is however expected given that the spread of simulated RTs was also randomly varied. Recovery of the LATER model parameter σ slightly underestimates the true value (Figure 6c). This is however expected given the sample size and using MLE as fitting procedure, a similar bias in σ is observed when fitting a normal distribution with MLE. Also expectedly, the IQR increases with the tested value of σ. Recovery of the race model parameter ρ is fairly unbiased in the median (Figure 6d). In contrast, the mean can be slightly biased, which is probably linked to the bounded nature of the parameter space (ρ is limited between -1 and 1). The IQR shows some large spikes especially for values of ρ close to 1. The issue here is that there is no or only a very small expected redundancy gain in these conditions and that there can be even a negative

Figure 6 ■ Parameter recovery. a) Using random parameterization, 250 versions of the context invariant race model were generated. From each version, 2,000 data sets were sampled, each with 100 trials per condition. The model was then fitted to the random samples to compare the parameter recovery with true simulation values. b-e) Recovery of μ_X, σ_X, ρ, and η (recovery of μ_Y and σ_Y is not shown as it matches μ_X and σ_X). The dashed line indicates identity of true values and recovered estimates. The interquartile range (IQR) as a measure of reliability is shown as a continuous surface to reduce clutter.
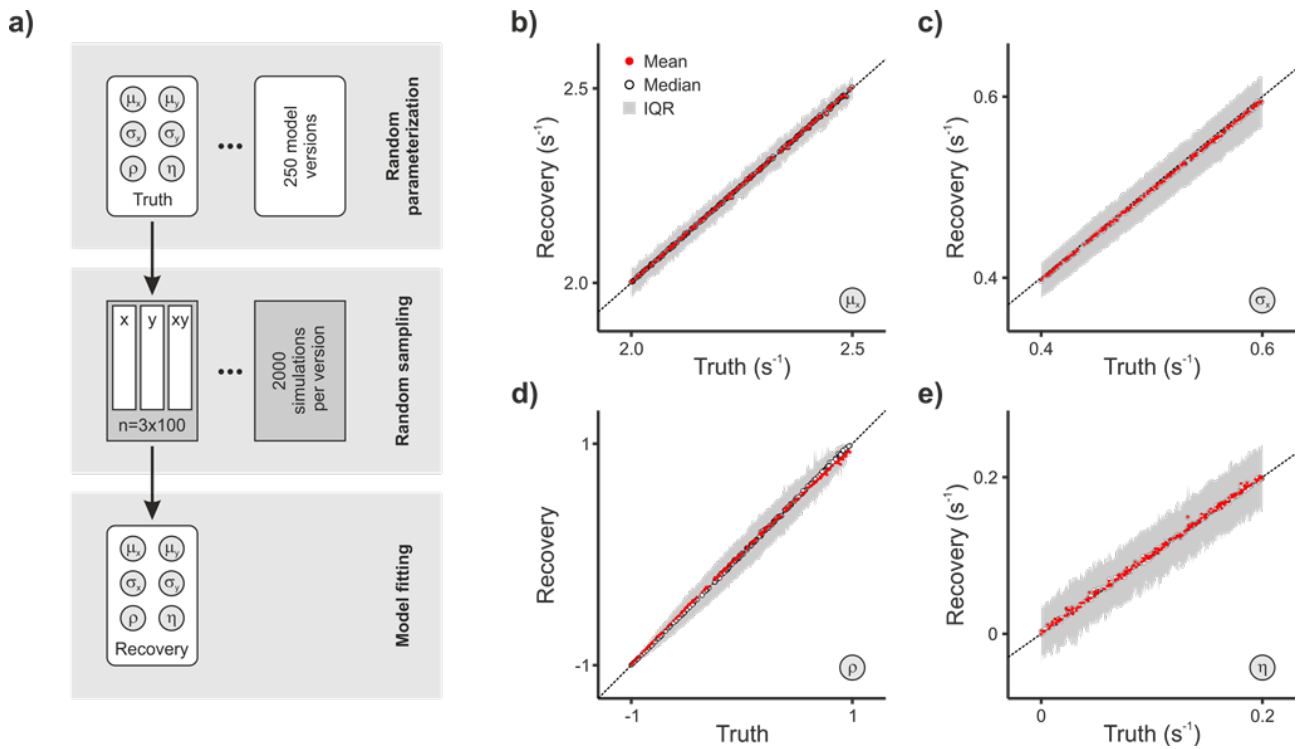
RSE in some random samples (meaning that responses in the redundant condition are slower than in the faster of the single signal conditions). Such effects enlarge when performance in the two single signal conditions is highly different (i.e., when the corresponding RT distributions hardly overlap). In such extreme situations, parameter recovery performance can be poor. This finding implies that caution should be taken if the model is used to analyse experiments that hardly yield redundancy gains. Finally, recovery of the race model parameter η is fairly unbiased except for a few model versions as just discussed with the parameter ρ (Figure 6e). In summary, the parameter recovery simulations validate the joint fitting procedures as introduced with the RSE-box, and show that the model introduced by Otto and Mamassian (2012) is in itself consistent given that simulated model parameter are recovered unbiased. The synthetic data here are of course very clean in the sense that they were generated by the model. The following simulations address some of the issues that can occur with real

data.

Error contamination and outlier correction

One important difference between synthetic and real data is that human performance, especially when tested in long-lasting experimental sessions, is prone to errors. In simple detection tasks, as frequently employed in RSE experiments, one issue is that participants respond on occasion in the absence of a target signal. The amount of such false alarms can be estimated by including catch trials in the experimental procedures. On signal trials, it is still not trivial to distinguish a genuine response from a false alarm that just happens to fall in the valid response window after signal onset (Ratcliff, 1993). Critically, it is well-established that such erroneous responses can mask violations of Miller's bound (Eriksen, 1988; Miller & Lopes, 1991). At least for this reason, it is expected that contamination with erroneous responses can bias parameter recovery.

Figure 7 ■ Error contamination and outlier correction. a) Recovery of σ_X. b) Recovery of η. To estimate the effect of erroneous responses (e.g., caused by false alarms falling in the valid response window after stimulus onset), an RSE experiment is simulated as in Figure 6 and then contaminated with 0-10% erroneous responses (randomly sampled between 0.2 and 0.3 s). Parameter recovery is performed without correction (None) or following a correction method using either the standard deviation (SD) or the median absolute deviation (MAD) as criterion. The dashed line indicates true parameter values. Recovery performance is based on 2,000 simulations per data point.
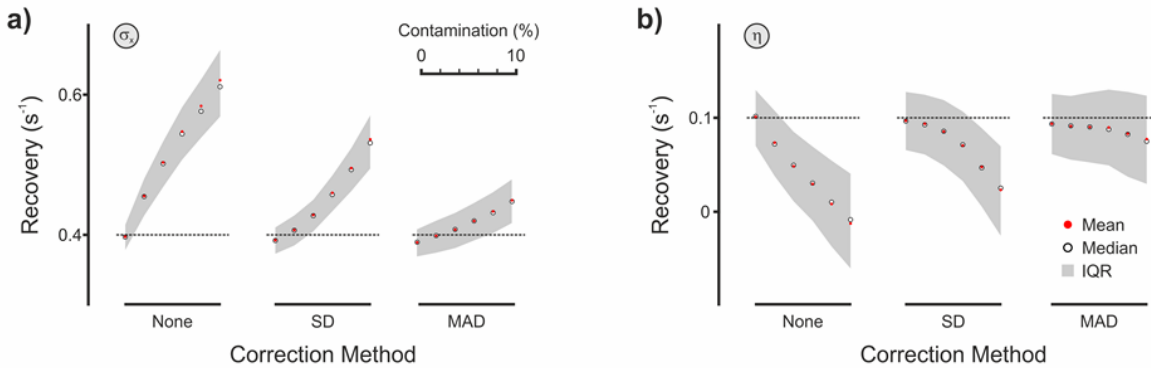
To simulate the effect of erroneous responses on parameter recovery, the RSE is here simulated with the model parameters as summarized in Table 2. Additionally, between 0% and 10% of the trials were replaced with synthetic erroneous responses. These responses were randomly sampled from a uniform distribution between 0.2 and 0.3 s (which is the time window just before or slightly overlapping with most genuine responses; for comparison with an uncontaminated sample, see Figure 2c). For each level of contamination, 2,000 synthetic data sets were generated. These data sets were then analysed using three procedures. First, no outlier correction was performed. Second, responses that deviated on the reciprocal scale (1/RT) by more than 3 SDs from the mean were removed from analysis. Third, responses that deviated on the reciprocal scale by more than 1.4826 x 3 MADs from the median were removed (which is implemented by the RSE-box function `outCorrect`, see section 'Defining RT distributions'). Both correction methods are equally conservative by excluding about 0.27% of the data points with uncontaminated samples. Both correction methods were applied separately in each RSE condition. With all three procedures, the data samples were then analysed using the function `fitRse` as in the parameter recovery simulation above.

If no outlier correction is performed, the key finding is that very few erroneous responses can heavily bias parameter recovery. Particularly affected are the LATER model parameter σ (Figure 7a) and the race model parameter η

(Figure 7b, see 'None'). With respect to the latter, the simulation is in agreement with earlier reports that fast erroneous responses can mask violations of Miller's bound (Eriksen, 1988; Miller & Lopes, 1991). In the model proposed by Otto and Mamassian (2012), violations are covered by the noise parameter η, which is underestimated in this simulation when synthetic data is contaminated with erroneous responses (the model does not predict violations of Miller's bound for values of η equal to or smaller than 0). It should be noted that this simulation generated erroneous responses that are always close to the genuine responses (in the time window between 0.2 and 0.3 s after stimulus onset). With erroneous responses occurring also in earlier time windows (e.g., between 0.1 and 0.2 s), the effect of very few erroneous responses on parameter recovery is even worse, which can lead in extreme cases to a failure of the model fitting procedures provided by the RSE-box (results not shown). The simulation of error contamination highlights that the model-based analysis approach, as presented here, requires a systematic data cleaning procedure.

If an outlier correction is performed, both tested correction methods reduce the bias in parameter recovery (Figure 7, see 'SD' and 'MAD'). Notably, the method based on median and MAD outperforms the correction based on mean and SD in that the bias due to error contamination is systematically smaller. The advantage of the outlier correction based on median and MAD is even larger

when more extreme erroneous responses are included in the simulation (e.g., between 0.1 and 0.2 s). In this case, the MAD method has basically no problems in removing extreme erroneous responses whereas recovery performance using the SD method deteriorates (results not shown). The poorer recovery performance of the outlier correction based on mean and SD is expected because these measures are particularly sensitive to outliers themselves, which makes the method based on median and MAD the recommended choice (Leys et al., 2013).

An alternative method to correct for erroneous responses, coined 'kill-the-twin', was developed in RSE research to be applied in tests of Miller's inequality (Eriksen, 1988; Miller & Lopes, 1991). The basic idea is that the timing of false alarms can be estimated based on performance in catch trials. Then, RT distributions in the three signal conditions are corrected using the false alarm distribution (for a recent discussion of the method, see Gondan & Minakata, 2016). One issue with this method is that false alarm rates are typically low, which implies that estimated false alarm distributions are unreliable. In the extreme, it is well possible that no false alarm is recorded in catch trials, yet a few erroneous responses have contaminated signal trials. The 'kill-the-twin' method provides in such cases no handle to remove even extreme outliers from the data, which can consequently bias parameter estimates. For this reason, the method based on median and MAD is preferred as a systematic and automatic outlier removal procedure before model-fitting.

Misfit in single signal conditions

Another important difference between synthetic and real data is that the true distribution type of RTs in the single signal conditions is unknown. When using the classic approach, this is not an issue because basic race model predictions, like Miller's bound (Equation 7), can be computed without making any assumptions about the distribution. In contrast, the model proposed by Otto and Mamassian (2012) assumes that RTs in the single signal conditions follow a reci-normal distribution, as predicted by the LATER model (Carpenter & Williams, 1995; Noorani & Carpenter, 2016). The parameter recovery simulation above shows that the fitting procedures yield unbiased parameter estimates when the distributional assumption is correct, but what if the assumption is incorrect?

To exemplify potential effects of an incorrect distributional assumption on parameter recovery, the RSE is here simulated using an independent race model (i.e., assuming both statistical independence and context invariance). In contrast to the previous simulations, responses to single signals X and Y were here sampled from an ex-Gaussian distribution (Heathcote et al., 1991; Luce, 1986).

Critically, with the arbitrarily specified parameters μ, σ, and τ as summarized in Table 3, the resulting distribution shape cannot be matched by a reci-normal distribution. To simulate responses to redundant signals XY on a given trial, the faster of two independent samples from the ex-Gaussian distributions was selected as response. Using this model, 2,000 synthetic data sets were generated, each with 100 RTs for each condition. Each sample was then analysed using the function fitRse as in the previous simulations.

When the distributional assumption made in the modelling approach is incorrect, parameter recovery can be biased (Table 3). There is of course no match between the parameters of the generating ex-Gaussian distribution and the parameter estimates of the fitted LATER model (although some parameter names use identical symbols). The key issue is that there is a bias in the best-fitting race model parameters. The simulation assumed both statistical independence and context invariance. Consequently, the race model parameters ρ should be zero to match statistical independence. The race model parameter η should also be zero (s^{-1}) because any other value would manifest a violation of context invariance. However, both parameters are different from zero, which indicates a bias in parameter recovery due to the incorrect distributional assumption. Such biases are likely to scale with the mismatch between true and assumed distribution type (which was here large given the arbitrarily selected ex-Gaussian distribution). This finding highlights that best-fitting model parameters should be interpreted with caution if the model fit in the single signal conditions shows a systematic mis-fit.

Vincent averages

A final issue is that an analysis based on RT distributions requires large sample sizes. As measurement time with human participants is often limited due to practical reasons (at least to avoid fatigue effects), it is tempting to collapse data from different subjects to obtain reliable group RT distributions. An undesired effect of simply pooling data across participants is that this method would inject variance from individual differences into the group distribution. An alternative is Vincent averaging (Ratcliff, 1979). In this method, equal numbers of quantile RTs are extracted for each participant. To obtain a group distribution, individual quantile RTs are then averaged at each rank. Vincent averaging has frequently been used in RSE research to inspect RT distributions (e.g., Miller, 1982) as well as the substrate in modelling approaches (e.g., Otto & Mamassian, 2012). However, Vincent averaging is not always appropriate (e.g., Cousineau, Thivierge, Harding, & Lacouture, 2016; Rouder & Speckman, 2004; Thomas & Ross, 1980), which questions whether the method is suitable in RSE research.

To test the effect of Vincent averaging on parame-

Table 3 ■ Parameter recovery with distributional mismatch.

Signal condition	Generating model	Parameter	Simulation, true value	Fitting model	Parameter	Recovery, best-fit
Single X	ex-Gaussian	μ_x	0.35 s	LATER model	μ_x	2.16 s^{-1}
		σ_x	0.02 s		σ_x	0.50 s^{-1}
		τ_x	0.15 s			
Single Y	ex-Gaussian	μ_Y	0.35 s	LATER model	μ_y	2.16 s^{-1}
		σ_y	0.02 s		σ_y	0.49 s^{-1}
		τ_y	0.15 s			
Redundant XY	Race model	Statistical independence		Race model	ρ	-0.092
		Context invariance			η	0.042 s^{-1}

Figure 8 ■ Vincent averages. a) Heterogeneous participants. Expected median RTs to single signals X and Y were sampled from a bivariate normal distribution for 200 simulated participants. RTs to redundant signals XY were sampled for each simulated participant using the independent race model. b) Group RT distributions using Vincent averaging. Miller's bound is computed based on the group distributions in the single signal conditions (the violation is quantified as introduced in Figure 3b). Each distribution is based on 50 RTs per participant, yielding 10,000 RTs in total.
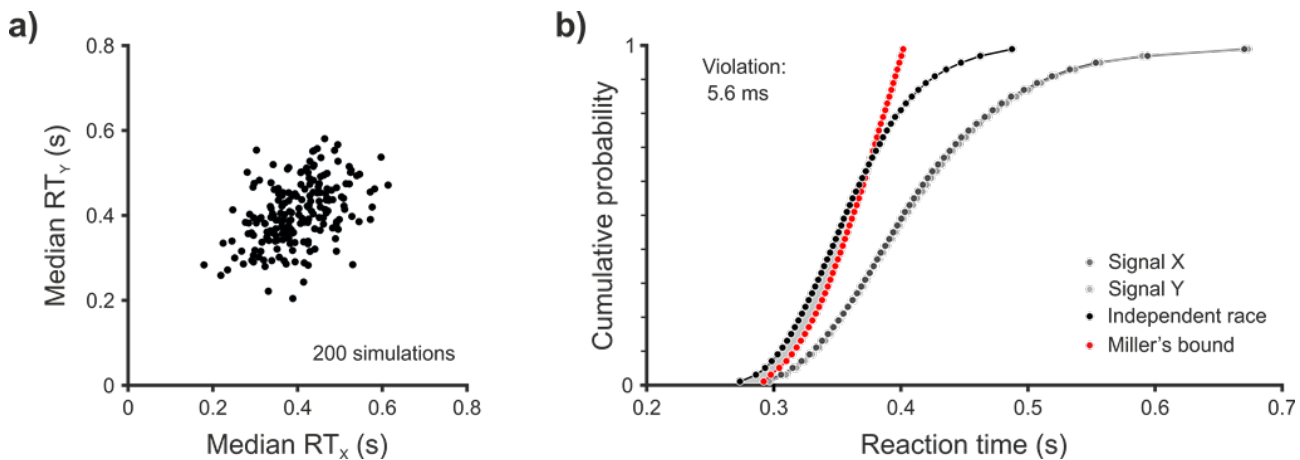
ter recovery, the RSE is here simulated with a heterogeneous group of participants (Figure 8a). For this, expected median RTs to single signals X and Y were randomly sampled from a bivariate normal distribution (mean$_{X,Y}$: 0.4 s, SD$_{X,Y}$: 0.08 s, correlation: 0.5). The corresponding value of the LATER model parameter μ is then given by the reciprocal of the expected median RT ($\mu = 1/medianRT$). The second LATER model parameter σ was held constant at 0.4 s^{-1} for both single signals and across participants. RTs to redundant signals XY were simulated using a race model under the assumptions of statistical independence and context invariance (i.e., the corresponding race model parameters ρ and η were both set to zero). The RSE-box function simRace was used to generate synthetic data for 200 participants with 50 RTs per condition. As a first analysis step, group RT distri-

butions were obtained using Vincent averaging (Ratcliff, 1979, each distribution is consequently based on 10,000 RTs). The group distributions were then analysed with respect to Miller's bound (Miller, 1982, using the RSE-box function getViolation) as well as using the model proposed by Otto and Mamassian (2012) (using the function fitRse as in the previous simulations).

The use of group RT distributions estimated by Vincent averaging can be misleading when analysing RSE experiments (Figure 8b). For example, Miller's bound (Equation 7) can be computed based on the group RT distributions as estimated in the single signal conditions. Inspection of the group RT distribution with redundant signals shows then a clear violation of Miller's bound. Hence, it seems justified to conclude that the effect cannot be explained by Raab's (1962) independent race model. The critical issue

is that the data was generated precisely by that model and that the violation of Miller's bound here is an artefact introduced by the averaging procedure. To avoid the issue, Miller's bound, and any other race model prediction, must be computed individually for each participant.

Given the result of the first analysis, it is no surprise that Vincent averaging leads also to biased parameter estimates when analysing RSE experiments. In the simulation here, the true value of both ρ and η was zero. Yet, fitting the model to the group RT distributions shown in Figure 8b returns biased estimates for both parameters ($\rho = -0.42$; $\eta = 0.072$ s^{-1}). In contrast, parameter averaging of individual fits with the same data yields unbiased estimates ($\rho = 0.01$; $\eta = 0.003$ s^{-1}). The bias in the group analysis scales with the RT heterogeneity that is introduced in the single signal conditions (results not shown). While it is likely that the parametrization here overestimated the RT heterogeneity as found in real data, the simulation still highlights that parameter averaging of individual fits is the recommended choice when modelling RSE experiments.

Conclusions and future development

The newly introduced RSE-box provides all functions that are needed to measure the size of the effect, to obtain basic race model predictions, or to check for violations of Miller's bound. By providing the toolbox, the intention is that the consistency of future RSE research can be improved, for example, by avoiding the frequent confusion of Raab's (1962) independent race model (Equation 6) and Miller's bound (Equation 7). Moreover, by using consistent tools and measures, a major aim is to support a comparative approach to understand differences across RSE experiments as recently initiated by Innes and Otto (2019). RSE research has so far produced an extraordinarily rich data set, which includes highly different subject populations with many clinical samples as well as a huge variability of signals. For example, the RSE can be observed both with signals within one sensory modality like vision and with signals across two modalities like vision and audition (e.g., Girard, Pelland, Lepore, & Collignon, 2013; Miller, 1982). Yet, how exactly processing interactions differ between uni- and multi-sensory stimulation remains to be investigated. Similarly, the basic redundant signals paradigm can be extended and tested with three redundant signals (Diederich & Colonius, 2004; Engmann & Cousineau, 2013; Todd, 1912), which invites for an extension of RSE-box in the near future. In general, while the RSE replicates reliably, a systematic analysis of differences across studies is lacking. Such analysis is ideally based on RT distributions, which may lead to a better understanding of interactions in the simultaneous processing of redundant signals.

An analysis of RT distributions becomes more informative if a model-based approach is used. However, the vast majority of RSE studies does unfortunately not provide testable models as an explanation of the effect, which is possibly one of the major weaknesses of the field. To overcome the issue, a central aim of the RSE-box is to make one of the very few models that explain the RSE at the level of RT distributions freely available and, thereby, to boost the use of models in research with redundant signals.

As a first step, the race model introduced by (Otto & Mamassian, 2012) can be used as a tool to study the processes and interactions underlying the RSE. Future research should here aim for a better understanding of the model parameters. For example, the correlation parameter ρ is linked to the sequential dependency of RTs in redundant signals experiments, which is likely to be a key factor for a full understanding of the effect. Likewise, the noise parameter η, which manifests a violation of the context invariance assumption, is strongly linked to violations of Miller's bound. By a systematic analysis of the two parameters across different sensory signals and experimental conditions, it may be possible to unveil more about the parameters and corresponding processing interactions.

As a second step, simulation studies can be very useful to validate model fitting procedures. The parameter recovery studies here show for example that the model introduced by Otto and Mamassian (2012) is in itself consistent as the fitting procedures yield unbiased parameter estimates (Figure 6). At present, it is the only model of the RSE that is published including such simulations. The parameter recovery studies further help to scrutinize analysis methods. For example, the simulations here demonstrate the need for a systematic outlier removal procedure, the importance to check for systematic mis-fit in the single signal conditions, as well as the inappropriateness of using Vincent averaging in the analysis of RTs with redundant signals. Moreover, simulations easily demonstrate that race models, if the context invariance assumption is dropped, are not limited by Miller's bound (Figure 3). In the end, the simulation tools may thus contribute in general to a better understanding of race models as an explanation of the RSE.

The ultimate goal of the RSE-box is to trigger model development. This may start directly with the race model introduced by Otto and Mamassian (2012), which explains violations of Miller's bound by a noise interaction. Yet, it is well possible that a differently modelled violation of the context invariance assumption provides better model fits. Likewise, there is the competing class of so-called coactivation models, which explain the RSE by a pooling of sensory evidence in a single decision unit (e.g., Diederich, 1995; Mordkoff & Yantis, 1991; Townsend & Wenger, 2004; Zehetleitner, Krummenacher, & Müller, 2009; ; for a review

covering this model class, see Colonius & Diederich, 2017). Future work should make these models equally available, for example, as part of an RSE-box extension. The availability of these models would then enable for the first time a direct comparison of the fundamentally different and competing approaches using objective measures of model selection, which would manifest a major improvement in RSE research.

Authors' note

References

Akaike, H. (1973). Information theory and an extension of the maximum likelihood principle. In B. N. Petrox & F. Caski (Eds.), *Second international symposium on information theory* (pp. 267–281). Budapest: Akademiai Kiado.

Amsellem, S., Hochenberger, R., & Ohla, K. (2018). Visual-olfactory interactions: Bimodal facilitation and impact on the subjective experience. *Chemical Senses*, *43*(5), 329–339. doi:10.1093/chemse/bjy018

Ashby, F. G., & Townsend, J. T. (1986). Varieties of perceptual independence. *Psychological Review*, *93*(2), 154–179. doi:10.1037//0033-295x.93.2.154

Bogacz, R. (2007). Optimal decision-making theories: Linking neurobiology with behaviour. *Trends in Cognitive Sciences*, *11*(3), 118–125. doi:10.1016/j.tics.2006.12.006

Carpenter, R. H. S., & Williams, M. L. (1995). Neural computation of log likelihood in control of saccadic eye movements. *Nature*, *377*(6544), 59–62. doi:10.1038/377059a0

Colonius, H. (1990). Possibly dependent probability summation of reaction-time. *Journal of Mathematical Psychology*, *34*(3), 253–275. doi:10.1016/0022-2496(90)90032-5

Colonius, H., & Diederich, A. (2006). The race model inequality: Interpreting a geometric measure of the amount of violation. *Psychological Review*, *113*(1), 148–154. doi:10.1037/0033-295X.113.1.148

Colonius, H., & Diederich, A. (2017). Formal models and quantitative measures of multisensory integration: A selective overview. *European Journal of Neuroscience*, *14*. doi:10.1111/ejn.13813

Cousineau, D., Thivierge, J. P., Harding, B., & Lacouture, Y. (2016). Constructing a group distribution from individual distributions. *Canadian Journal of Experimental Psychology*, *70*(3), 253–277. doi:10.1037/cep0000069

Crosse, M. J., Foxe, J. J., & Molholm, S. (2019). Developmental recovery of impaired multisensory processing in autism and the cost of switching sensory modality. *bioRxiv*, *1*. doi:10.1101/565333

Diederich, A. (1995). Intersensory facilitation of reaction-time - evaluation of counter and diffusion coactivation models. *Journal of Mathematical Psychology*, *39*(2), 197–215. doi:10.1006/jmps.1995.1020

Diederich, A., & Colonius, H. (2004). Bimodal and trimodal multisensory enhancement: Effects of stimulus onset and intensity on reaction time. *Perception & Psychophysics*, *66*(8), 1388–1404. doi:10.3758/Bf03195006

Efron, B., & Tibshirani, R. J. (1994). An introduction to the bootstrap: CRC press.

Engmann, S., & Cousineau, D. (2013). Triple redundant signals effect in the visual modality. *Universitas Psychologica*, *12*(5), 1473–1491. doi:10.11144/Javeriana.UPSY12-5.trse

Eriksen, C. W. (1988). A source of error in attempts to distinguish coactivation from separate activation in the perception of redundant targets. *Perception & Psychophysics*, *44*(2), 191–193. doi:10.3758/Bf03208712

Fitousi, D., & Algom, D. (2018). A system factorial technology analysis of the size congruity effect: Implications for numerical cognition and stochastic modeling. *Journal of Mathematical Psychology*, *84*, 57–73. doi:10.1016/j.jmp.2018.03.006

Forstmann, B. U., Ratcliff, R., & Wagenmakers, E. J. (2016). Sequential sampling models in cognitive neuroscience: Advantages, applications, and extensions. *Annual Review of Psychology*, *67*, 641–666. doi:10.1146/annurev-psych-122414-033645

Freeman, L. C. A., Wood, K. C., & Bizley, J. K. (2018). Multisensory stimuli improve relative localisation judgments compared to unisensory auditory or visual stimuli. *Journal of the Acoustical Society of America*, *143*(6), El516–El522. doi:10.1121/1.5042759

Girard, S., Pelland, M., Lepore, F., & Collignon, O. (2013). Impact of the spatial congruence of redundant targets on within-modal and cross-modal integration. *Experimental Brain Research*, *224*(2), 275–285. doi:10.1007/s00221-012-3308-0

Gold, J. I., & Shadlen, M. N. (2007). The neural basis of decision making. *Annual Review of Neuroscience*, *30*, 535–574. doi:10.1146/annurev.neuro.29.051605.113038

Gondan, M. (2010). A permutation test for the race model inequality. *Behavior Research Methods*, *42*(1), 23–28. doi:10.3758/BRM.42.1.23

Gondan, M., Lange, K., Rösler, F., & Röder, B. (2004). The redundant target effect is affected by modality switch costs. *Psychonomic Bulletin & Review*, *11*(2), 307–313. doi:10.3758/Bf03196575

Gondan, M., & Minakata, K. (2016). A tutorial on testing the race model inequality. *Attention, Perception, & Psychophysics*, *78*(3), 723–735. doi:10.3758/s13414-015-1018-y

Grice, G. R., Canham, L., & Gwynne, J. W. (1984). Absence of a redundant-signals effect in a reaction-time task with divided attention. *Perception & Psychophysics*, *36*(6), 565–570. doi:10.3758/Bf03207517

Heathcote, A., Brown, S. D., & Wagenmakers, E. J. (2015). An introduction to good practices in cognitive modeling. In B. U. Forstmann & E.-J. Wagenmakers (Eds.), *An introduction to model-based cognitive neuroscience* (pp. 25–48). New York: Springer.

Heathcote, A., Brown, S., Wagenmakers, E. J., & Eidels, A. (2010). Distribution-free tests of stochastic dominance for small samples. *Journal of Mathematical Psychology*, *54*(5), 454–463. doi:10.1016/j.jmp.2010.06.005

Heathcote, A., Popiel, S. J., & Mewhort, D. J. K. (1991). Analysis of response-time distributions - an example using the stroop task. *Psychological Bulletin*, *109*(2), 340–347. doi:10.1037//0033-2909.109.2.340

Hélie, S. (2006). An introduction to model selection: Tools and algorithms. *Tutorials in Quantitative Methods for Psychology*, *2*(1), 1–10.

Innes, B. R., & Otto, T. U. (2019). A comparative analysis of response times shows that multisensory benefits and interactions are not equivalent. *Scientific Reports*, *9*, 2921–2922. doi:10.1038/s41598-019-39924-6

Kiesel, A., Miller, J., & Ulrich, R. (2007). Systematic biases and type i error accumulation in tests of the race model inequality. *Behavior Research Methods*, *39*(3), 539–551.

Kinchla, R. A. (1974). Detecting target elements in multielement arrays: A confusability model. *Perception & Psychophysics*, *15*(1), 149–158. doi:10.3758/BF03205843

Leys, C., Ley, C., Klein, O., Bernard, P., & Licata, L. (2013). Detecting outliers: Do not use standard deviation around the mean, use absolute deviation around the median. *Journal of Experimental Social Psychology*, *49*(4), 764–766. doi:10.1016/j.jesp.2013.03.013

Luce, R. D. (1986). *Response times: Their role in inferring elementary mental organization*. New York: Oxford University Press.

Lunn, J., Sjoblom, A., Ward, J., Soto-Faraco, S., & Forster, S. (2019). Multisensory enhancement of attention depends on whether you are already paying attention. *Cognition*, *187*, 38–49. doi:10.1016/j.cognition.2019.02.008

Miller, J. (1982). Divided attention: Evidence for coactivation with redundant signals. *Cognitive Psychology*, *14*(2), 247–279. doi:10.1016/0010-0285(82)90010-X

Miller, J. (1986). Timecourse of coactivation in bimodal divided attention. *Perception & Psychophysics*, *40*(5), 331–343. doi:10.3758/Bf03203025

Miller, J., & Lopes, A. (1991). Bias produced by fast guessing in distribution-based tests of race models. *Perception & Psychophysics*, *50*(6), 584–590. doi:10.3758/Bf03207544

Mordkoff, J. T., & Yantis, S. (1991). An interactive race model of divided attention. *Journal of Experimental Psychology: Human Perception and Performance*, *17*(2), 520–538. doi:10.1037/0096-1523.17.2.520

Myung, I. J. (2003). Tutorial on maximum likelihood estimation. *Journal of Mathematical Psychology*, *47*(1), 90–100. doi:10.1016/S0022-2496(02)00028-7

Nadarajah, S., & Kotz, S. (2008). Exact distribution of the max/min of two Gaussian random variables. *IEEE Transactions on Very Large Scale Integration (VLSI) Systems*, *16*(2), 210–212. doi:10.1109/tvlsi.2007.912191

Noorani, I., & Carpenter, R. H. (2016). The later model of reaction time and decision. *Neuroscience and Biobehavioral Reviews*, *64*, 229–251. doi:10.1016/j.neubiorev.2016.02.018

Otto, T. U., Dassy, B., & Mamassian, P. (2013). Principles of multisensory behavior. *Journal of Neuroscience*, *33*(17), 7463–7474. doi:10.1523/JNEUROSCI.4678-12.2013

Otto, T. U., & Mamassian, P. (2012). Noise and correlations in parallel perceptual decision making. *Current Biology*, *22*(15), 1391–1396. doi:10.1016/j.cub.2012.05.031

Otto, T. U., & Mamassian, P. (2017). Multisensory decisions: The test of a race model, its logic, and power. *Multisensory Research*, *30*(1), 1–24. doi:10.1163/22134808-00002541

Pitt, M. A., & Myung, I. J. (2002). When a good fit can be bad. *Trends in Cognitive Sciences*, *6*(10), 421–425. doi:10.1016/S1364-6613(02)01964-2

Raab, D. H. (1962). Statistical facilitation of simple reaction times. *Transactions of the New York Academy of Sciences*, *24*(5), 574–590.

Ratcliff, R. (1979). Group reaction-time distributions and an analysis of distribution statistics. *Psychological Bulletin*, *86*(3), 446–461. doi:10.1037/0033-2909.86.3.446

Ratcliff, R. (1993). Methods for dealing with reaction-time outliers. *Psychological Bulletin*, *114*(3), 510–532. doi:10.1037/0033-2909.114.3.510
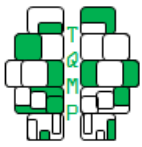
Rouder, J. N., & Speckman, P. L. (2004). An evaluation of the vincentizing method of forming group-level response time distributions. *Psychonomic Bulletin & Review*, *11*(3), 419–427. doi:10.3758/Bf03196589

Schwarz, G. E. (1978). Estimating the dimension of a model. *Annals of Statistics*, *6*(2), 461–464. doi:10.1214/aos/1176344136

Stefanou, M. E., Dundon, N. M., Bestelmeyer, P. E. G., Koldewyn, K., Saville, C. W. N., Fleischhaker, C., & Klein, C. (2019). Electro-cortical correlates of multisensory integration using ecologically valid emotional stimuli: Differential effects for fear and disgust. *Biological Psychology*, *142*, 132–139. doi:10.1016/j.biopsycho.2019.01.011

Thomas, E. A. C., & Ross, B. H. (1980). On appropriate procedures for combining probability-distributions within the same family. *Journal of Mathematical Psychology*, *21*(2), 136–152. doi:10.1016/0022-2496(80)90003-6

Todd, J. (1912). *Reaction to multiple stimuli (vol. 3)*. New York City: The Science Press.

Townsend, J. T., & Wenger, M. J. (2004). A theory of interactive parallel processing: New capacity measures and predictions for a response time inequality series.

Psychological Review, *111*(4), 1003–1035. doi:10.1037/0033-295x.111.4.1003

Ulrich, R., Miller, J., & Schröter, H. (2007). Testing the race model inequality: An algorithm and computer programs. *Behavior Research Methods*, *39*(2), 291–302. doi:10.3758/Bf03193160

Vrancken, L., Vermeulen, E., Germeys, F., & Verfaillie, K. (2019). Measuring facial identity and emotion integration using the redundancy gain paradigm. *Attention, Perception, & Psychophysics*, *81*(1), 217–236. doi:10.3758/s13414-018-1603-y

Yang, C. T., Altieri, N., & Little, D. R. (2018). An examination of parallel versus coactive processing accounts of redundant-target audiovisual signal processing. *Journal of Mathematical Psychology*, *82*, 138–158. doi:10.1016/j.jmp.2017.09.003

Zehetleitner, M., Krummenacher, J., & Müller, H. J. (2009). The detection of feature singletons defined in two dimensions is based on salience summation, rather than on serial exhaustive or interactive race architectures. *Attention, Perception, & Psychophysics*, *71*(8), 1739–1759. doi:10.3758/App.71.8.1739

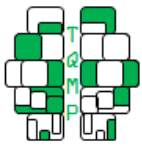## Appendix A: An example of appendix

The following code example shows the RSE-box function `demo01_quantiles`, which performs the analysis steps depicted in Figure 2 and Figure 3. To illustrate functionality, synthetic data generated by RSE-box functions is used. The code can be easily adapted to analyse empirical data. Similarly, the functions `demo02_later` and `demo03_race` illustrate analysis steps as depicted in Figure 4 and Figure 5, respectively. Table 1 provides an overview of RSE-box functions.

```
function demo01_quantiles
    % DEMO01_QUANTILES  Demonstration of the RSE−box: Basic RT analysis
    %
    % DEMO01_QUANTILES demonstrates the functionality of key functions  in  the  RSE toolbox  in
    % four steps:  (1)  Simulation  of a redundant signals  experiment.  (2)  Plotting  of
    % cumulative distribution  functions .  (3)  Measuring  the  redundancy gain  (the  speed−up
    % of reaction  times  in  the  redundant compared to  the  single  signal  conditions ).
    % (4) Estimating  violations  of  Miller 's  bound. Documentation of  exemplified  toolbox
    % functions can be  obtained  using  the  HELP function.
    %
    % See also: simRace, getCP, getGrice , getGain, getMiller ,  getViolation ,  fillArea

    % Copyright (C) 2017−18 Thomas Otto, University  of  St  Andrews
    % See rseBox_license  for   details

    % −−−−−−−−−−−−−−−−−−−−−−−−−−−−−−−−−−−−−−−−−−−−−−−−−−−−−−−−−−−
    % (1) Simulate  RSE
    % −−−−−−−−−−−−−−−−−−−−−−−−−−−−−−−−−−−−−−−−−−−−−−−−−−−−−−−−−−−

    % Sample size ( trials  per  condition )
    n = 50;
```

```matlab
% LATER model parameters to simulate the  single  signal  conditions
mu     = [ 2.5,  2.5 ];
sigma = [ 0.4,  0.4 ];

% Race model parameters to simulate  the  redundant  signals   condition
% (set both parameters  to  0  for  the  independent  race  model)
rho = -0.5;
eta =  0.1;

% Simulate RSE experiment using a  race  model
data = simRace( n, mu, sigma, rho, eta );

% Get cumulative  probabilities
p = getCP( n );

% ------------------------------------------------------------
% (2) Plot  cumulative  distribution   functions
% ------------------------------------------------------------

% Figure size
figSize = [0.25 0.25 0.5 0.6];

% Open new figure
figure( 'units', 'normalized', 'outerposition', figSize )
hold on

% X-axis limits (min,  max)
xLim = [ 0.1 0.7 ];

% Colors for the  three  conditions  (green,  blue,  black)
color = 'gbk';
grey = [0.8 0.8 0.8];

% Plot RSE data (as  quantiles )
lh = zeros(1,3);
for ii=1:3
    lh(ii) = plot( data(:,ii), p, ['-o' color(ii)], 'MarkerSize', 7, ...
        'MarkerFaceColor', 'w' );
end

% Info text  and figure  format
legendText = { 'Signal 1', 'Signal 2', 'Redundant'};
figFormat( xLim, lh, legendText )
drawnow;

% ------------------------------------------------------------
% (3) Measuring redundancy gain
% ------------------------------------------------------------

% Open new figure
figure( 'units', 'normalized', 'outerposition', figSize )
hold on
```

```matlab
% Take Grice's bound as reference
grice = getGrice( data(:,1:2) );

% Redundancy gain
gain = getGain( data );
gain = round( gain, 3, 'significant' );

% Plot data
fillArea( [ data(:,3), grice ] );
for ii=1:2
    plot( data(:,ii), p, '-o', 'Color', grey, 'MarkerSize', 7,
        'MarkerFaceColor', 'w' );
end
lh(1) = plot( grice,      p, '-or', 'MarkerSize', 7, 'MarkerFaceColor', 'w' );
lh(2) = plot( data(:,3), p, '-ok', 'MarkerSize', 7, 'MarkerFaceColor', 'w' );

% Info text and figure format
text( 0.05, 0.90, 'Redundancy gain', 'units', 'normalized')
text( 0.05, 0.85, [num2str(gain) ' s'], 'FontWeight', 'bold',
    'units', 'normalized')
legendText = { 'Grice bound', 'Redundant'};
figFormat(xLim, lh(1:2), legendText)
drawnow;

% ---------------------------------------------------------------
% (4) Violation of Miller's bound
% ---------------------------------------------------------------

% Open new figure
figure( 'units', 'normalized', 'outerposition', figSize )
hold on

% Take Miller's bound as reference
miller = getMiller( data(:,1:2) );

% Violation area
violation = getViolation( data );
violation = round( violation, 3, 'significant' );

% Plot data
for ii=1:2
    plot( data(:,ii), p, '-o', 'Color', grey, 'MarkerSize', 7,
        'MarkerFaceColor', 'w' );
end
fillArea( [ data(:,3), miller ], [], 1 );
lh(1) = plot( miller,     p, '-or', 'MarkerSize', 7, 'MarkerFaceColor', 'w' );
lh(2) = plot( data(:,3), p, '-ok', 'MarkerSize', 7, 'MarkerFaceColor', 'w' );

% Info text and figure format
text( 0.05, 0.90, 'Violation area', 'units', 'normalized')
text( 0.05, 0.85, [num2str(violation) ' s'], 'FontWeight', 'bold',
```

```matlab
        'units', 'normalized')
    legendText = { 'Miller bound', 'Redundant'};
    figFormat( xLim, lh(1:2), legendText )

end




% ------------------------------------------------------------
% Figure formating
% ------------------------------------------------------------

function figFormat( xLim, lh, legendText )
    % General figure settings
    xlabel( 'Reaction time (s)', 'FontWeight', 'bold' )t
    ylabel( 'Cumulative probability', 'FontWeight', 'bold' )
    legend( lh, legendText, 'Location', 'southeast' )
    legend( 'boxoff' )
    set( gca, 'xlim', xLim, 'ylim', [0 1] )
end
```

Open practices

⬡ The *Open Material* badge was earned because supplementary material(s) are available on the journal's web site.

Citation

Otto, T. U. (2019). Rse-box: An analysis and modelling package to study response times to multiple signals. *The Quantitative Methods for Psychology*, *15*(2), 112–133. doi:10.20982/tqmp.15.2.p112